Pergamon

Int. J. Heat Mass Transfer. Vol. 37, Suppl. 1, pp. 233–239, 1994

0017–9310/94 $6.00 + 0.00

0017–9310(93)E0069–S

The thermal-hydraulics of aseptic food processing

M. MILLIES, D. DREW and R. T. LAHEY, JR.

Center for Multiphase Flow, Rensselaer Polytechnic Institute, Troy, NY 12180, U.S.A.

Abstract—The temperature profile for an N-component mixture of particles in a fluid flowing through a heated tube has been evaluated using a numerical method for the fluid and an analytical solution for the particles. The results for the time-at-temperature of the particles depend on the drift-flux parameters, which quantify the local slip. In particular, the more slip the better the heat transfer and the shorter the heat exchanger required for aseptic food processing. Two diagrams are given, which cover all parameters of interest for laminar flow.

1. INTRODUCTION

INDUSTRIAL food processing is the primary means of transferring food from the producer to the consumer in industrialized countries. The process of distributing and selling processed food may require months of stability of the food product. Bacterial contamination is normally suppressed by chemical additives, sterilization of the product or storing the product at low temperatures. The law requires that the sterilized product contains less than a certain number density of a target microorganism, for example *C. botulinum* spores in low acid foods. The spore lethality curve normally follows a first order decay, where the exponent depends mainly on temperature. Therefore, for product sterilization, each part of the food product has to be held at a given temperature for a specified time period. While this is easy to fulfill in batch processes, i.e. canning, it is more difficult to prove in continuous aseptic food processing, where sterilization takes place during flow through a heat exchanger. This paper presents the theoretical basis for predicting the needed length of a continuous flow food sterilizer when the flow rate, physical properties of the various components and the required holding time are given.

2. DRIFT-FLUX MODELS

Drift-flux models have been widely used to predict the volume fractions of two phases when the volumetric fluxes of each phase is known. The original work on drift-flux models was down by Zuber and Findlay [1] and Wallis [2]. Bhaga and Weber [3] have extended drift-flux models to the three-phase flow of solid, liquid and gas. Açiköz *et al.* [4] applied a similar drift-flux model to the three-phase flow of oil, water and air. Recently Millies *et al.* [5] developed a drift-flux model for N-component flow. The drift-flux equations become for N-component flow,

$$\frac{\langle j_k \rangle}{\langle \alpha_k \rangle} = C_{k,f}\langle j_t \rangle + V_{k,f}; \quad k = 1, \ldots N, \tag{1}$$

where, $C_{k,f}$ denotes the distribution parameter,

$$C_{k,f} \equiv \frac{\langle \alpha_k j_t \rangle}{\langle \alpha_k \rangle \langle j_t \rangle}, \tag{2}$$

$V_{k,f}$ denotes the drift velocity,

$$V_{k,f} \equiv \frac{\langle j_k - \alpha_k j_t \rangle}{\langle \alpha_k \rangle}. \tag{3}$$

It should be noted that the angular brackets denote cross sectional averaging and the drift-flux parameters $C_{k,f}$ and $V_{k,f}$ must be obtained from measurements.

3. CALCULATION OF THE TEMPERATURE FIELD FOR THE STERILIZATION PROCESS

The energy equation of a fluid containing food particles, for fully developed flow through a pipe, where axial conduction has been neglected, is:

$$\rho_f c_{pf} u_f(r) \frac{\partial T}{\partial z} = -\frac{1}{r}\frac{\partial}{\partial r}\left(\lambda_f [1 + \varepsilon_q(r)] r \frac{\partial T}{\partial r}\right) - \sum_k \varepsilon_{pk} \frac{6}{D_{p,k}} \alpha_{pk}(T - T_{pk,s}). \tag{4}$$

$\rho_f c_{pf}$ and λ_f denote the fluid density, heat capacity and heat conductivity, ε_{pk}, $D_{p,k}$, α_{pk} and $T_{pk,s}$ are the particle volume fraction, Sauter mean diameter, heat transfer coefficient and surface temperature of particle k, respectively, and $\varepsilon_q(r)$ is the turbulent diffusivity for heat.

Laminar flow is to be expected for continuous sterilization in most cases. So $\varepsilon_q(r)$ may be set equal zero. Nevertheless the option for turbulent flow has been implemented in the computational program. The results presented in this paper are restricted to laminar flow since the number of parameters increases considerably for turbulent flow. The temperature field inside the particle was evaluated assuming a spherical shape for the particles, since this is the worst case for heat transfer to the center of a particle. An energy balance for the particle gives

NOMENCLATURE

a	thermal diffusivity, equation (5)
c_{pf}	heat capacity, equation (4)
$C_{k,f}$	distribution parameter, equation (2)
$D_{p,k}$	Sauter mean diameter of particle of component k, equation (4)
j	volumetric flux, equation (1)
m	factor, giving the phase distribution of the particles, equation (17a)
n	exponent, giving the velocity profile of the liquid, equation (17b)
r	radial coordinate, equation (4)
R	radius of the tube, equation (17b)
t	time, equation (5)
T	temperature, equation (4)
u_f	axial velocity, equation (4)
$V_{k,f}$	drift velocity, equation (3)
z	axial coordinate, equation (4).

Greek symbols

α_{pk}	heat transfer coefficient particle/fluid, equation (4)
ε_q	turbulent diffusivity, equation (4)
$\varepsilon_{p,k}$	volume fraction of particles of component k, equation (4)
ζ	factor, equation (16)
κ_k	parameter, equation (11)
λ	thermal conductivity, equation (4)
$\lambda_{i,k}$	eigenvalue, equation (9).

Indices

f	fluid
k	component k
p	particle
t	total fluid and particles
*	dimensionless.

Numbers

Bi_k	Biot number, $(\alpha_k D_{p,k})/\lambda_k$
Pr_f	Prandtl number, ν_f/a_f
Re_f	Reynolds number of the fluid, $u_f D/\nu_f$
κ_k	parameter, $(a_p/D_{p,k}^2)(D^2/a_f)$.

$$\frac{\partial T_{p,k}}{\partial t} = a_{p,k}\nabla^2 T_{p,k}. \tag{5}$$

The boundary condition at the particle surface is

$$\lambda_k \left.\frac{\partial T_{p,k}}{\partial r}\right|_{r=D_{p,k}/2} = \alpha_k (T - T_{p,k}|_{r=D_{p,k}/2}). \tag{6}$$

We may define the Biot number as

$$Bi_k \equiv \frac{\alpha_k D_{p,k}}{\lambda_k}. \tag{7}$$

Equation (5) was solved analytically using separation of the variables, assuming spherical symmetry of the temperature field inside the particle. The analytical solution is

$$T_{p,k}(r^*, t^*) = T_{p,k}(r^*, 0) + \frac{Bi_k}{2r^*}\sum_i \frac{\sin(\lambda_{i,k})\sin(\lambda_{i,k}r^*)\lambda_{i,k}}{\lambda_{i,k} - \sin(\lambda_{i,k})\cos(\lambda_{i,k})}$$
$$\times (\kappa_k \lambda_{i,k}^2)\int_0^{t^*} e^{-\kappa_k \lambda_{i,k}^2 (t^* - \tau)}(T - T_{p,k}(r^*, 0))\,d\tau, \tag{8}$$

where Bi_k is the Biot number of particle k, and the eigenvalues $\lambda_{i,k}$ are obtained from

$$\lambda_{i,k} = \left(1 - \frac{Bi_k}{2}\right)\tan(\lambda_{i,k}). \tag{9}$$

The radial coordinate may be made dimensionless with the particle's radius and the dimensionless time coordinate is

$$t^* = t a_f / D^2, \tag{10}$$

where D denotes the tube diameter and a_f is the thermal diffusivity of the fluid. It is convenient to define κ_k as

$$\kappa_k \equiv 4\frac{a_p}{D_{p,k}^2}\frac{D^2}{a_f}, \tag{11}$$

where a_p denotes the thermal diffusivity of the particle.

Equations (4) and (8) were evaluated numerically in the z-direction using a constant temperature as the boundary condition at the tube wall. The surface temperature of the particles, which is required in equation (4), was evaluated from the numerical quadrature of equation (8).

4. THE NUMERICAL SOLUTION

The convergence of the sum in equation (8) is quite slow. So the first 50 eigenvalues are considered. Higher eigenvalues still give a contribution, but they reached their final value quickly compared to the time scale for heat transfer in the fluid. We note that

$$\lim_{t^* \to \infty} (\kappa_k \lambda_{i,k}^2)\int_0^{t^*} e^{-\kappa_k \lambda_{i,k}^2 (t^* - \tau)} 1\,d\tau = 1. \tag{12}$$

Thus the final value of the higher eigenvalues is given by

$$T_{p,k}(r^*, t^*) = T + \frac{Bi_k}{2r^*}\sum_i \frac{\sin(\lambda_{i,k})\sin(\lambda_{i,k}r^*)\lambda_{i,k}}{\lambda_{i,k} - \sin(\lambda_{i,k})\cos(\lambda_{i,k})}$$
$$\times \left[(\kappa_k \lambda_{i,k}^2)\int_0^{t^*} e^{-\kappa_k \lambda_{i,k}^2 (t^* - \tau)}(T - T_{p,k}(r^*, 0))\,d\tau - (T - T_{p,k}(r^*, 0))\right]. \tag{13}$$

This equation gave good convergence for all calculations presented here. While stability is no challenge for the analytical solution just presented, it is

for the numerical solution of the temperature field in the liquid. The time scale required for the analytical solution varies widely with the diameter and heat conductivity of the particle. Therefore up to 10 000 steps for the temperature field in the liquid were required while one step was sufficient for the temperature field inside the particle. The intermediate results for the temperature in the liquid are cancelled after each step for the particle temperature, since they are of no further interest during the calculation.

The numerical calculations are performed on an AIX/370 parallel processor. The computer code was vectorized in order to speed up the computation. It was found from dimensional analysis that it was sufficient to vary four parameters in order to cover all possible combinations of parameters. More than a thousand calculations were performed with different sets of these four parameters. The results presented in the next section are based on these results.

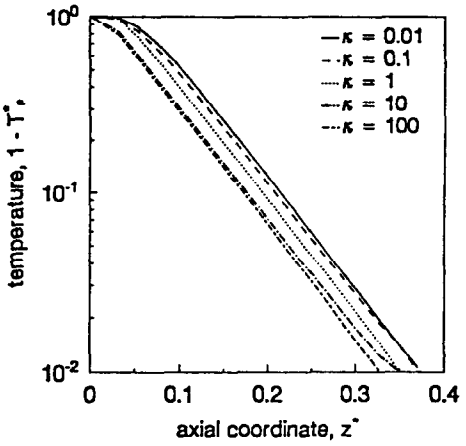

FIG. 2. Temperature in the center of a particle as a function of axial location in the tube for various κ ($C_{p,f} = 1.0$, $V^*_{p,f} = 0.0$, $\varepsilon_p \to 0$).

5. RESULTS OF THE NUMERICAL CALCULATION

The temperature at the center of a particle, shown in Fig. 1, depends on the location of the particle in the tube.

As expected, the particles at the center of the tube are the coldest, and thus the most limiting during the sterilization process. The nondimensional temperature at the center of the particles located on the axis of the tube is given by:

$$T^*_{p,i} \equiv \frac{T_{p,i} - T_{p,e}}{T_w - T_{p,e}}, \tag{14}$$

where T_w is the temperature of the tube wall and $T_{p,e}$ the particle temperature at the entrance of the tube. Typical results are given in Fig. 2. The axial coordinate was made dimensionless with

$$z^* \equiv \frac{z}{Re_f Pr_f D} \Big/ \left(1 + \left(3.0 \frac{a_f D^2_{p,k}}{a_p D^2}\right)^4\right)^{0.25}. \tag{15}$$

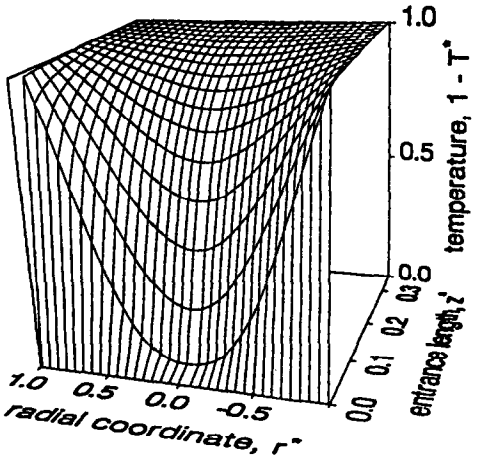

FIG. 1. Temperature in the center of a particle ($\kappa = 1$, $C_{p,f} = 1.0$, $V^*_{p,f} = 0$, $\varepsilon_p \to 0$).

Equation (15) implies that the required length of the sterilization section is dependent on properties of the fluid and the particles. The definition given in equation (15) makes sense only for monodispersed particles, so that only one value for the particle diameter, $D_{p,k}$, exists. We will have to redefine the nondimensional axial coordinate for the case of polydispersed particles. The particle temperature rapidly becomes equal to the temperature of the fluid for small values of $(a_f D^2_{p,k})/(a_p D^2)$, that is, for small particles compared to the tube diameter, or high thermal diffusivity in the particle compared to the fluid. In contrast, the heat transfer in the particles is much slower than in the fluid if $(a_f D^2_{p,k})/(a_p D^2)$ is large. The dimensionless axial coordinate, z^*, also corresponds to a time scale

$$z^* \equiv \frac{t/(\zeta \bar{u})}{Re_f Pr_f D} \Big/ \left(1 + \left(3.0 \frac{a_f D^2_{p,k}}{a_p D^2}\right)^4\right)^{0.25}, \tag{16}$$

where t is the residence time of the particle in the heated tube. The factor ζ is introduced into equation (16) since the FDA currently requires the fastest moving particle velocity to be twice the mean velocity (i.e. $\zeta = 2.0$). This corresponds to laminar Newtonian flow, which is considered to be the worst case, since most food's rheological behavior is dilatant. The required length of the sterilization section may be found as follows: the axial coordinate, z^*, where the particle's center reaches the required temperature for sterilization, may be evaluated from Fig. 2, then the tube length giving the required holding time may be calculated from equation (16), and then these lengths are added. Normally, an adiabatic holding section is used to achieve sterilization. In order to use the drift-flux parameters to determine the effect of local slip, we may assume that the relative velocity of the particles with respect to the fluid is independent of the radial position of the particle and that the radial distribution

of the volume fraction for the particles and the fluid velocity is given by:

$$\varepsilon_{p,k}(r) = \varepsilon_{p,k}(0)[1+m(1-2(r/R)^2)], \quad (17a)$$

$$u_f(r) = u_f(0)[1-(r/R)^n]. \quad (17b)$$

The relative velocity of the particles and the parameters n and m in equations (17a) and (17b) can then be evaluated from the definitions of the drift-flux parameters, equations (2) and (3).

The temperature at the center of a particle is shown in Fig. 3, with drift velocity as a parameter. The drift velocity quantifies the local relative velocity of the particles with respect to the fluid. The thermal boundary layer becomes thinner, and the heat transfer to the particle improves, as the relative velocity increases. Two limiting cases can be seen in Fig. 3; the heat transfer to the particle is lower, and thus the required length of the holding section is longer for small drift velocities. The second limit is obtained for very high drift velocities. For this case the thermal resistance through the boundary layer becomes small as does the required length of the holding section. The influence of the volume fraction on the particles is shown in Fig. 4. The heat transfer is reduced for large volume fractions of the particles since the heat transfer to the particles decreases the fluid temperature. The influence of the distribution parameter is shown in Fig. 5. A value of unity for the distribution parameter corresponds to a uniform distribution over the cross sectional area of the tube. Values between 0.9 and 1.1 may be expected for the sterilization process since the differences of the densities between particles and fluid is normally small. It can be seen in Fig. 5 that the effect of the distribution parameter depends on whether the particles are concentrated in the center of the pipe ($C_{p,f} > 1.0$) or near the wall ($C_{p,f} < 1.0$). The food will be heated in the heating section to nearly the wall temperature before it enters the holding section. Only small values of $1-T^*_{p,k}$ are therefore important for design purposes. We note that for small values of $1-T^*_{p,k}$ the curves become straight lines in Figs. 2–4. It is therefore sufficient to predict the slope $\partial \log_{10}(1-T^*_{p,k})/\partial z^*$ and the horizontal intercept, z^*_0. The temperature of the particle's center may then be calculated from

$$\log_{10}(1-T^*_{p,k}) = \left|\frac{\partial \log_{10}(1-T^*_{p,k})}{\partial z^*}\right|(z^*-z^*_0). \quad (18)$$

We redefine z^* here for simplicity, since the influence of the parameter κ will have to be considered in several locations:

$$z^* \equiv \frac{z}{Re_f Pr_f D}. \quad (19)$$

The full numerical solution and equation (18) are

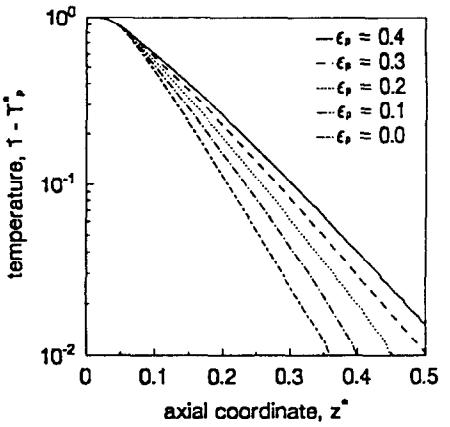

FIG. 4. Temperature at the particle's center as a function of axial location in the tube; parameter: volume fraction of the particles ($\kappa = 1$, $V^*_{p,f} = 0$, $C_{p,f} = 1.0$).

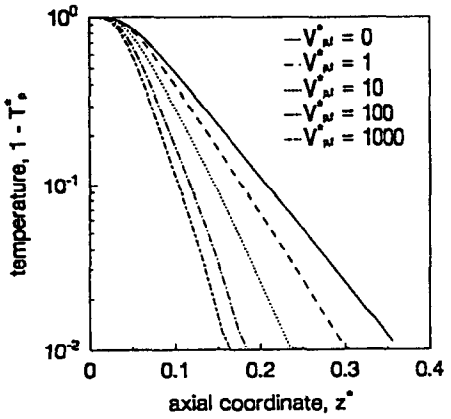

FIG. 3. Temperature of the particle's center as a function of axial location in the tube; parameter: dimensionless drift velocity, $V^*_{p,f} = (V_{p,f}D_{p,k})/\nu_f$, ($\kappa = 1$, $C_{p,f} = 1.0$, $\varepsilon_p \to 0$).

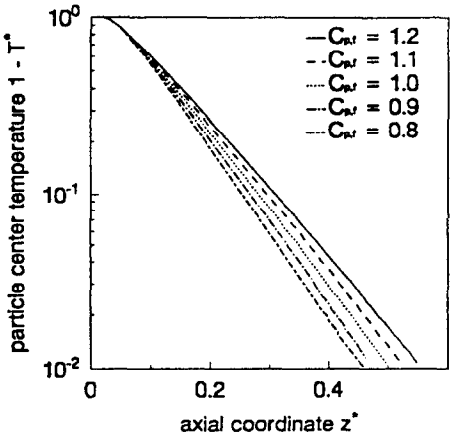

FIG. 5. Temperature at the particle's center as a function of axial location in the tube; parameter: distribution parameter, ($\kappa = 1$, $V^*_{p,f} = 0$, $\varepsilon_p = 0.3$).

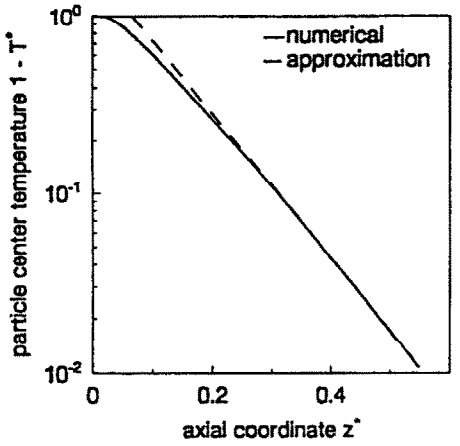

FIG. 6. Temperature at the particle's center as a function of axial location in the tube, the approximation against the numerical solution ($\kappa = 1$, $V^*_{p,f} = 0$, $\varepsilon_p = 0.3$, $C_{p,f} = 1.2$).

shown in Fig. 6 for comparison. We note that the only deviation is for small z^*. Figure 7 contains the same information required for design purposes, but it is obvious that a higher information density is now possible. Our goal is to present the dependency of slope and intercept from all parameters in one graph, if possible. In order to do this, we need to reduce the number of parameters, since only two paramters can be shown in one plot. We find, that the distribution parameter has its influence only via the volume fraction and that the volume fraction of the particles only appears in one place in the differential equations. Moreover, the influence of the distribution parameter disappears for small volume fractions. Therefore we may summarize the influence of both the distribution parameter and the volume fraction in one new parameter. Most of the particles are distributed near the wall of the tube if the distribution parameter becomes zero, as can be seen from equation (2). These particles have negligible influence on the heat transfer to the center of the flow, since they are quickly heated due to their small distance from the heated wall. The influence of the volume fraction disappears therefore if the distribution parameter becomes zero. Therefore we may try $(\varepsilon_{p,k} C^x_{p,f})$ as a new parameter. We obtain a very good fit for the exponent, $x = 2.44$.

It can be shown from dimensional analysis of the differential equations that only three parameters are sufficient: the Biot number, the parameter κ, containing the ratio of tube and particle diameter and the ratio of the thermal conductivities, and the term, $\varepsilon_{p,k} C^{2.44}_{p,f} Nu_{p,k} (D/D_{p,k})^2$. Let us now summarize the influence of the Biot number and the parameter κ. The limiting cases are as follows.

1. The parameter κ becomes zero, which means the thermal conductivity of the particle is negligibly small or the particle is very big; in both cases the slope becomes zero.
2. The Biot number becomes zero, which corresponds to a bad heat transfer through the boundary layer of the particle and the slope becoming zero.
3. The Biot number becomes very large. For this case the temperature at the surface of the particle is essentially the same as the temperature of the fluid surrounding the particle. The slope then depends only on the parameter κ and not on the Biot number.
4. The parameter κ becomes very large. The heat transfer inside of the particle becomes very good in this case. It can be shown, that the slope then depends only on the product of the Biot number and the parameter κ.

These limiting cases may be fulfilled if the slope depends on the parameter $\kappa/(y + 1/Bio)$ instead of both the Biot number and the parameter κ separately. We obtain a very good fit for the coefficient, $y = 0.059$.

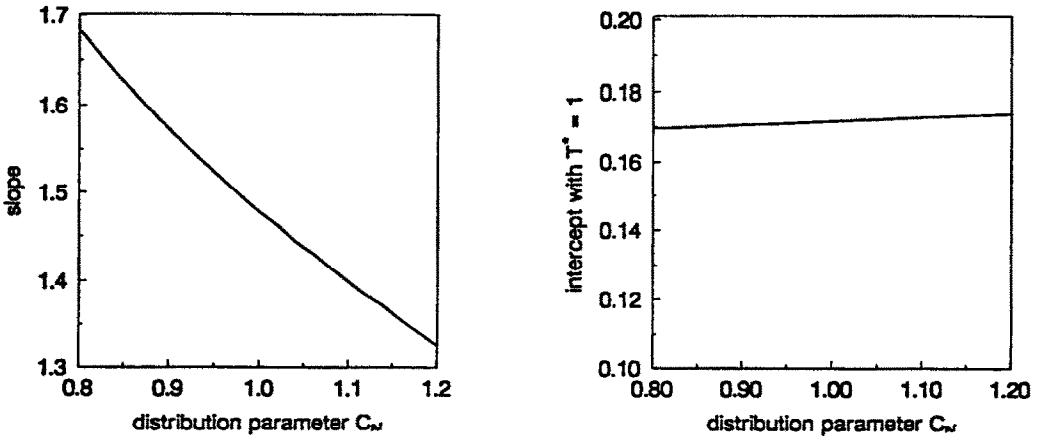

FIG. 7. Temperature at the particle's center as a function of axial location in the tube, the approximation against the numerical solution ($\kappa = 1$, $V^*_{p,f} = 0$, $\varepsilon_p = 0.3$, $C_{p,f} = 1.2$).

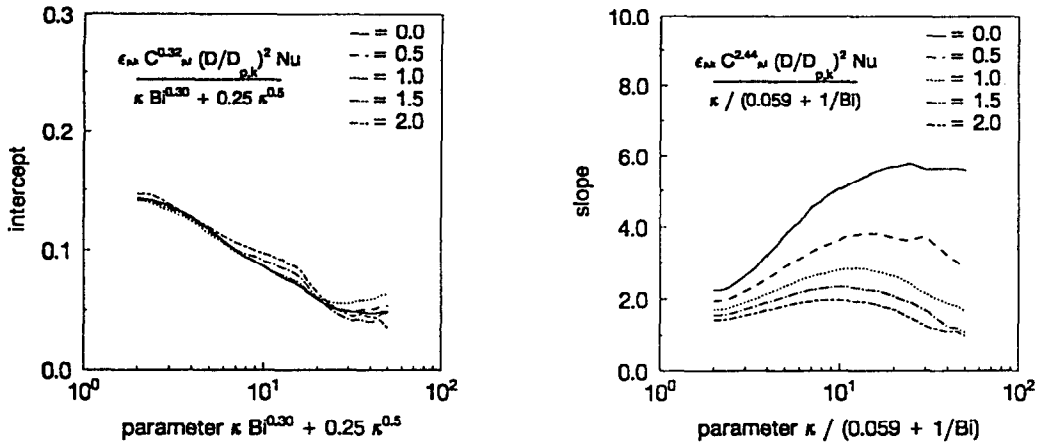

FIG. 8. Intercept and slope as a function of distribution parameter ($\kappa = 1$, $V^*_{p,f} = 0$, $\varepsilon_p = 0.3$).

Next we describe the horizontal intercept, z_0^*, which signifies the time lag required for the heat to pass through the fluid and reach the particles. The distribution parameter and the volume fraction of the particles may be included in one parameter, $\varepsilon_{p,k} C_{p,f}^{0.32} Nu_{p,k} (D/D_{p,k})^2$. We note that the exponent of the distribution parameter is different now. Nearly all particles have to be heated up before the heat transfer reaches the particles in the center of the flow. The distribution of the particles does not affect that much, therefore the influence of the distribution parameter on the intercept is small. The Biot number and the parameter κ may be included in one parameter, if we regard again the limiting cases. The heat flux to a particle is proportional to κBio if the Biot number is small. It is proportional to $\kappa^{0.5}$ for large values of the Biot numbers, where the heat transfer resistance of the boundary layer becomes negligible. A good fit is given by, $\kappa Bio^{0.30} + 0.25\kappa^{0.5}$.

Thus the influence of all parameters can be presented in two figures, given in Fig. 8.

In order to obtain these graphs we needed to interpolate in two dimensions between 1218 calculated points. This caused some of the curves to not be completely smooth. As can be seen in Fig. 8(a), the intercept is virtually independent of the second parameter, which includes the volume fraction of the particles. We may conclude that the delay until the heat transfer affects particles in the center of the flow is caused only by heating up the fluid and by the thermal resistance inside and outside the particle, but not by other particles surrounding the particle under consideration. Let us now discuss the slope.

1. For very few ($\varepsilon_{p,k} \to 0$) and very small particles ($\kappa \to \infty$) we obtain that only the heat transfer through the fluid is of importance. This limiting value for the slope can be calculated from $Nu = 3.66$ to be *slope* = 6.4 in agreement with Fig. 8.

2. For very few ($\varepsilon_{p,k} \to 0$) but very large particles ($\kappa \to 0$) the heat transfer through the particle towards its center becomes limiting. This corresponds to a straight line in the half logarithmic scale of Fig. 8.

3. If there are many particles ($\varepsilon_{p,k} > 0$) the slope becomes smaller the more particles there are and the better the heat transfer becomes towards them.

We have assumed up to now that only one kind of particle was present. The temperatures at the particle's center for three different classes of particles are shown in Fig. 9. It is obvious that the particles with the smallest value of κ_k (which are the biggest particles with the smallest heat conductivity) are the most limiting for continuous flow sterilization. For comparison, the temperature in the particle's center is also shown when only monodispersed particles are present, but with the same volume fraction as all three classes

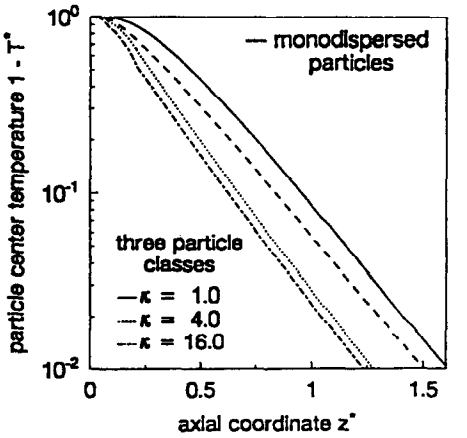

FIG. 9. Temperature of the particle's center for monodispersed particles ($\kappa = 1$, $\varepsilon_{p,t} = 0.3$) and for three classes of particles (different values for κ, the biggest particles correspond to the smallest value of κ, $\varepsilon_{p,k} = 0.1$ for each class) ($V^*_{p,f} = 0$, $C_{p,f} = 1$).

together. It is remarkable that the slope of the temperature inside the biggest particles versus entrance length becomes essentially the same in all cases. This slope just corresponds to an eigenvalue, which is valid for the whole system of particles and the fluid. The intercept is bigger for multiple particles compared to the same volume fraction of monodispersed particles. This is because the smaller particles are heated up first before significant heat is transferred to the big particles in the center of the flow.

6. SUMMARY AND CONCLUSIONS

The temperature profile for an N-component flow of particles in a fluid through a heated tube has been calculated numerically for the fluid and using an analytical solution for the particles. The results for the time-at-temperature of the particles depend on the drift-flux parameters. In particular, the more slip the better the heat transfer, and the shorter the heat exchanger required for aseptic food processing. The results are presented in a compact way, which allows us to present the influence of all parameters in two diagrams for laminary flow.

REFERENCES

1. N. Zuber and J. A. Findlay, Average volumetric concentration in two-phase flow systems, *J. Heat Transfer* 453–468 (1965).
2. G. B. Wallis, *One Dimensional Two-Phase Flow*. Wiley, New York (1969).
3. D. Bhaga and M. E. Weber, Holdup in vertical two and three phase flow, Part I and II, *Can. J. Chem. Engng* **50,** 323–328 (1972).
4. M. Açiköz *et al.*, Global volumetric phase fractions in horizontal three-phase flows, *A.I.Ch.E. Jl* **38,** 1049–1058 (1992).
5. M. Millies *et al.*, The analysis of aseptic food processing using N-component drift-flux techniques, *Proc. IHTC-10*, August (1994).